Table S1. Overview of misfit functions that are applied in each experiment type.

	RMSE	VolRMSE	BasinRMSE	VarRMSE	RMAE	BasinRMAE
TWIN	✓					
TWIN_IDP	✓					
synObs_ALL_noise	✓					
synObs_IDP_noise	✓	✓		✓		
synObs_ALL_seas	✓	✓			✓	
synObs_IDP+_seas	✓					
synObs_IDP_seas	✓	✓	✓		✓	✓
synObs_ALL_circ	✓	✓			✓	
synObs_IDP+_circ	✓				✓	✓
synObs_IDP_circ	✓	✓	✓		✓	✓

Table S2. Overview of the optimisation results (parameter values obtained with the best individual in the last generation, its misfit, and the globally integrated Zn uptake flux, as well as the total number of iterations until a termination criterion was reached and the misfit calculated with reference parameter values). Numbers specified in percentage refer to the relative difference from the reference parameter values or the reference misfit, and are coloured in red or blue when they underestimate or overestimate the corresponding value by more than 10% respectively.

Experiment type	Misfit metric	a_{Zn} (-)	b_{Zn} (µM)	c_{Zn} (µM^{-1})	L (µM)	Number of iterations	$M_{reference}$ (µM) or (µM$^{1/2}$) or (-)	$M_{optimised}$ (µM) or (µM$^{1/2}$) or (-)	Globally integrated Zn export flux (Mmol yr^{-1})
reference		6.00×10^{-3}	3.00×10^{-5}	0.320	1.20×10^{-3}				27.085
TWIN_ALL	RMSE	6.00×10^{-3}	3.00×10^{-5}	0.320	1.20×10^{-3}	126		4.483E-09	27.085
		-0.01%	+0.03%	+0.12%	-0.03%				0.00%
TWIN_IDP	RMSE	6.00×10^{-3}	3.00×10^{-5}	0.320	1.20×10^{-3}	153		2.310E-09	27.085
		0.00%	+0.01%	-0.02%	-0.01%				0.00%
synObs_ALL_noise	RMSE	6.19×10^{-3}	2.89×10^{-5}	0.182	1.38×10^{-3}	95	2.207×10^{-4}	2.205×10^{-4}	27.019
		+3.14%	-3.68%	-42.98%	+15.16%			-0.07%	-0.24%
synObs_IDP_noise	RMSE	6.10×10^{-3}	3.87×10^{-5}	0.160	1.02×10^{-3}	185	1.728×10^{-4}	1.727×10^{-4}	27.058
		+1.74%	+28.90%	-50.00%	-15.08%			-0.04%	-0.10%
synObs_IDP_noise	VolRMSE	6.23×10^{-3}	3.54×10^{-5}	0.160	1.14×10^{-3}	118	2.187×10^{-4}	2.186×10^{-4}	27.072
		+3.76%	+17.85%	-50.00%	-4.86%			-0.07%	-0.05%
synObs_IDP_noise	VarRMSE	7.43×10^{-3}	1.36×10^{-5}	0.160	3.39×10^{-3}	200	9.549×10^{-1}	9.913×10^{-1}	27.117
		+23.78%	-54.55%	-50.00%	+182.60%			+3.81%	0.12%
synObs_ALL_seas	RMSE	6.87×10^{-3}	4.79×10^{-5}	0.160	1.35×10^{-3}	200	2.183×10^{-4}	2.128×10^{-4}	26.820
		+14.50%	+59.70%	-50.00%	+12.24%			-2.49%	-0.98%
synObs_ALL_seas	VolRMSE	7.77×10^{-3}	2.20×10^{-5}	6.962	3.75×10^{-3}	106	1.944×10^{-4}	1.786×10^{-4}	26.540
		+29.45%	-26.65%	+2075.63%	+212.50%			-8.09%	-2.01%
synObs_ALL_seas	RMAE	6.72×10^{-3}	4.08×10^{-5}	0.179	1.27×10^{-3}	200	1.071×10^{-2}	1.049×10^{-2}	27.025
		+12.01%	+35.98%	-43.96%	+5.77%			-2.08%	-0.22%
synObs_IDP+_seas	RMSE	6.37×10^{-3}	2.89×10^{-5}	0.619	1.69×10^{-3}	51	1.731×10^{-4}	1.703×10^{-4}	26.881
		+6.09%	-3.51%	+93.54%	+40.66%			-1.59%	-0.75%
synObs_IDP_seas	RMSE	5.86×10^{-3}	2.19×10^{-5}	1.428	1.83×10^{-3}	55	1.619×10^{-4}	1.585×10^{-4}	26.897
		-2.37%	-26.84%	+346.14%	+52.12%			-2.13%	-0.69%
synObs_IDP_seas	VolRMSE	4.88×10^{-3}	1.07×10^{-5}	7.042	2.80×10^{-3}	90	1.875×10^{-4}	1.644×10^{-4}	26.733
		-18.62%	-64.47%	+2100.63%	+133.23%			-12.35%	-1.30%
synObs_IDP_seas	RMAE	6.50×10^{-3}	2.94×10^{-5}	0.184	1.45×10^{-3}	200	8.349×10^{-3}	8.237×10^{-3}	27.093

		+8.40%	-1.99%	-42.37%	+21.00%			-1.35%	0.03%
synObs_IDP_seas	BasinRMSE	6.60×10^{-3}	5.70×10^{-5}	0.160	9.81×10^{-4}	200	7.673×10^{-4}	7.407×10^{-4}	26.950
		+10.07%	+89.96%	-50.00%	-18.26%			-3.47%	-0.50%
synObs_IDP_seas	BasinRMAE	6.63×10^{-3}	5.32×10^{-5}	0.160	9.76×10^{-4}	200	4.610×10^{-2}	4.456×10^{-2}	27.043
		+10.52%	+77.43%	-50.00%	-18.71%			-3.34%	-0.15%
synObs_ALL_circ	RMSE	7.00×10^{-3}	6.00×10^{-5}	0.160	1.35×10^{-3}	143	1.311×10^{-3}	1.303×10^{-3}	26.596
		+16.70%	+100.00%	-50.00%	+12.71%			-0.66%	-1.80%
synObs_ALL_circ	VolRMSE	6.00×10^{-4}	6.00×10^{-5}	7.050	1.39×10^{-3}	68	4.580×10^{-3}	1.367×10^{-3}	23.072
		-90.00%	+100.00%	+2103.13%	+15.45%			-70.15%	-14.82%
synObs_ALL_circ	RMAE	6.10×10^{-3}	3.86×10^{-5}	0.162	1.09×10^{-3}	76	2.652×10^{-2}	2.651×10^{-2}	26.964
		+1.71%	+28.57%	-49.33%	-9.04%			-0.04%	-0.44%
synObs_IDP+_circ	RMSE	6.19×10^{-3}	6.00×10^{-5}	0.162	9.30×10^{-4}	134	1.162×10^{-3}	1.155×10^{-3}	26.761
		+3.10%	+99.86%	-49.52%	-22.46%			-0.63%	-1.20%
synObs_IDP+_circ	RMAE	5.17×10^{-3}	1.13×10^{-5}	2.074	3.75×10^{-3}	81	2.661×10^{-2}	2.636×10^{-2}	26.065
		-13.77%	-62.39%	+548.23%	+212.26%			-0.95%	-3.76%
synObs_IDP+_circ	BasinRMAE	5.91×10^{-3}	6.00×10^{-5}	0.160	1.12×10^{-3}	121	1.498×10^{-1}	1.491×10^{-1}	26.354
		-1.56%	+100.00%	-50.00%	-6.90%			-0.45%	-2.70%
synObs_IDP_circ	RMSE	6.14×10^{-3}	6.00×10^{-5}	0.160	9.41×10^{-4}	94	1.180×10^{-3}	1.173×10^{-3}	26.722
		+2.36%	+100.00%	-50.00%	-21.60%			-0.65%	-1.34%
synObs_IDP_circ	VolRMSE	6.00×10^{-4}	6.00×10^{-5}	7.050	1.73×10^{-3}	78	1.291×10^{-3}	1.152×10^{-3}	22.117
		-90.00%	+100.00%	+2103.13%	+44.53%			-10.80%	-18.34%
synObs_IDP_circ	RMAE	4.06×10^{-3}	3.62×10^{-5}	0.160	8.99×10^{-4}	66	2.674×10^{-2}	2.630×10^{-2}	25.842
		-32.36%	+20.78%	-50.00%	-25.08%			-1.65%	-4.59%
synObs_IDP_circ	BasinRMSE	6.28×10^{-3}	6.00×10^{-5}	0.160	1.45×10^{-3}	113	7.021×10^{-3}	6.936×10^{-3}	26.136
		+4.61%	+100.00%	-50.00%	+20.48%			-1.21%	-3.50%
synObs_IDP_circ	BasinRMAE	5.58×10^{-3}	6.00×10^{-5}	0.160	1.01×10^{-3}	106	1.507×10^{-1}	1.500×10^{-1}	26.316
		-7.03%	+100.00%	-50.00%	-16.06%			-0.47%	-2.84%

Table S3. Description and results of additional optimisation.

Parent experiment	Misfit metric	Adaption	a_{Zn}	b_{Zn}	c_{Zn}	L	Number of iterations	M_{parent}	$M_{optimised}$	Globally integrated Zn uptake flux
			(-)	(μM)	(μM^{-1})	(μM)		($\mu M^{1/2}$)	($\mu M^{1/2}$)	(Mmol yr^{-1})
synObs_IDP_circ	RMAE (Eq. 5 in main text)	$w_{i,j}$ obtained from $nObs_j$ in synObs_IDP+_circ when distinguishing between five ocean basins (see main text)	4.28×10^{-3}	5.37×10^{-5}	0.161	6.95×10^{-4}	182	2.630×10^{-2}	2.640×10^{-2}	25.953

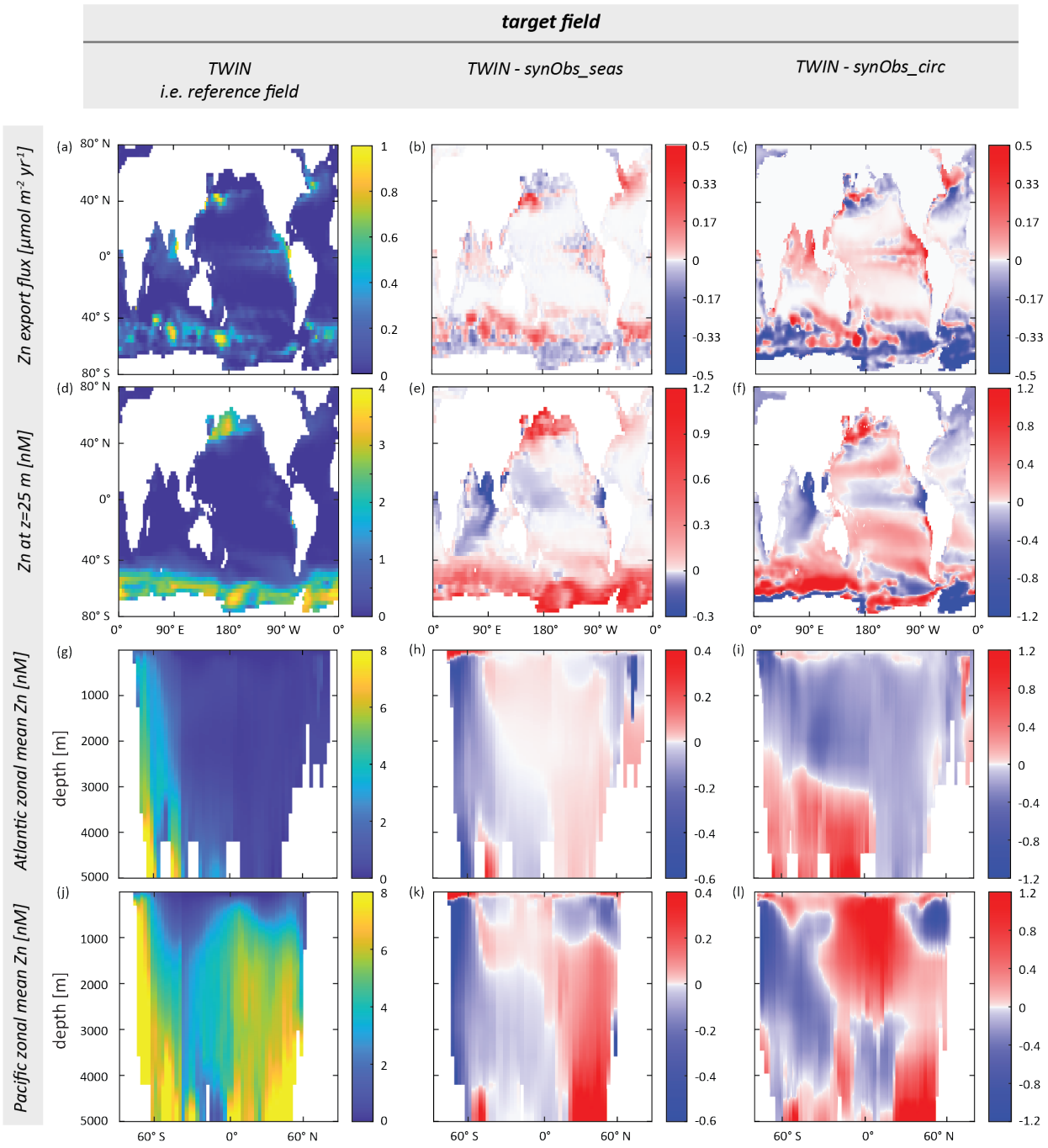

Figure S1. Maps of surface Zn concentration [nM] (first row), and zonal mean Zn concentration for the Atlantic (second row) and the Pacific (third row), showing the reference Zn field (first column), the difference between this field and the target field in synObs_seas (second column) and synObs_circ (third column) experiments.

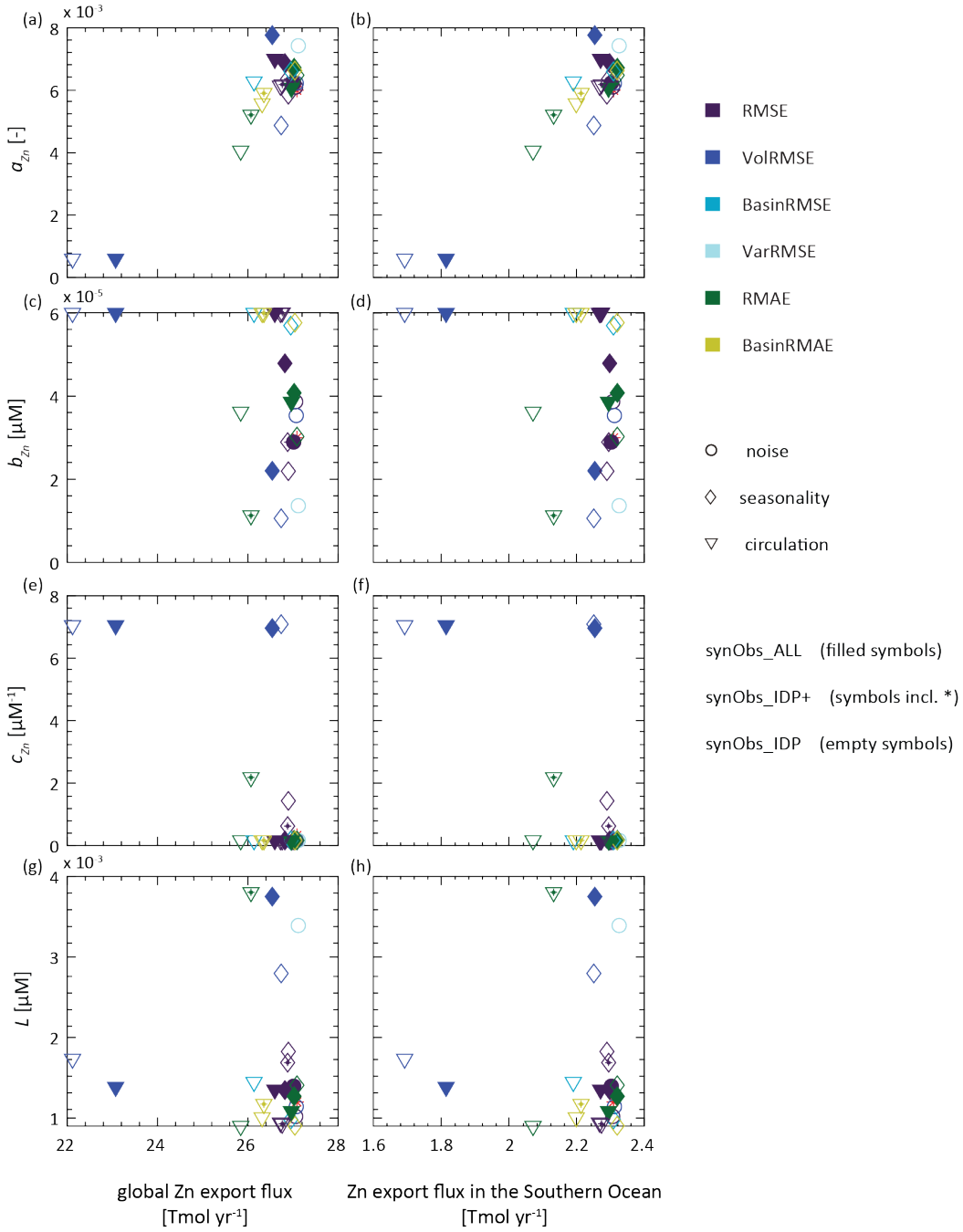

Figure S2. Zn export flux integrated globally (first column) and over the Southern Ocean (>50° S; second column) versus optimised parameter values from synObs experiments.

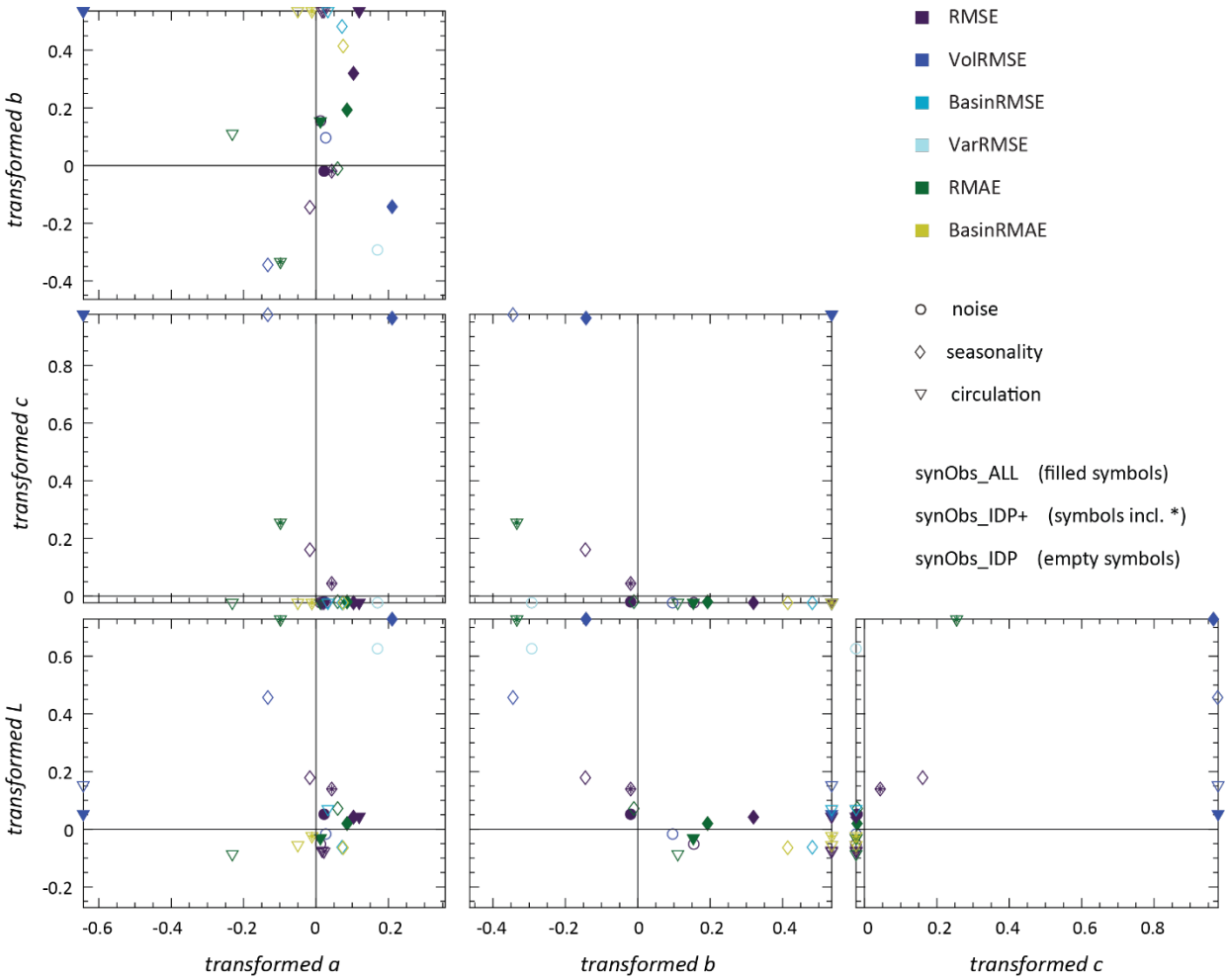

Figure S3. Relationship between optimised parameter values. Parameter values are transformed by rescaling each parameter space to an interval of unit length, and shifting this space such that zero corresponds to the reference value.

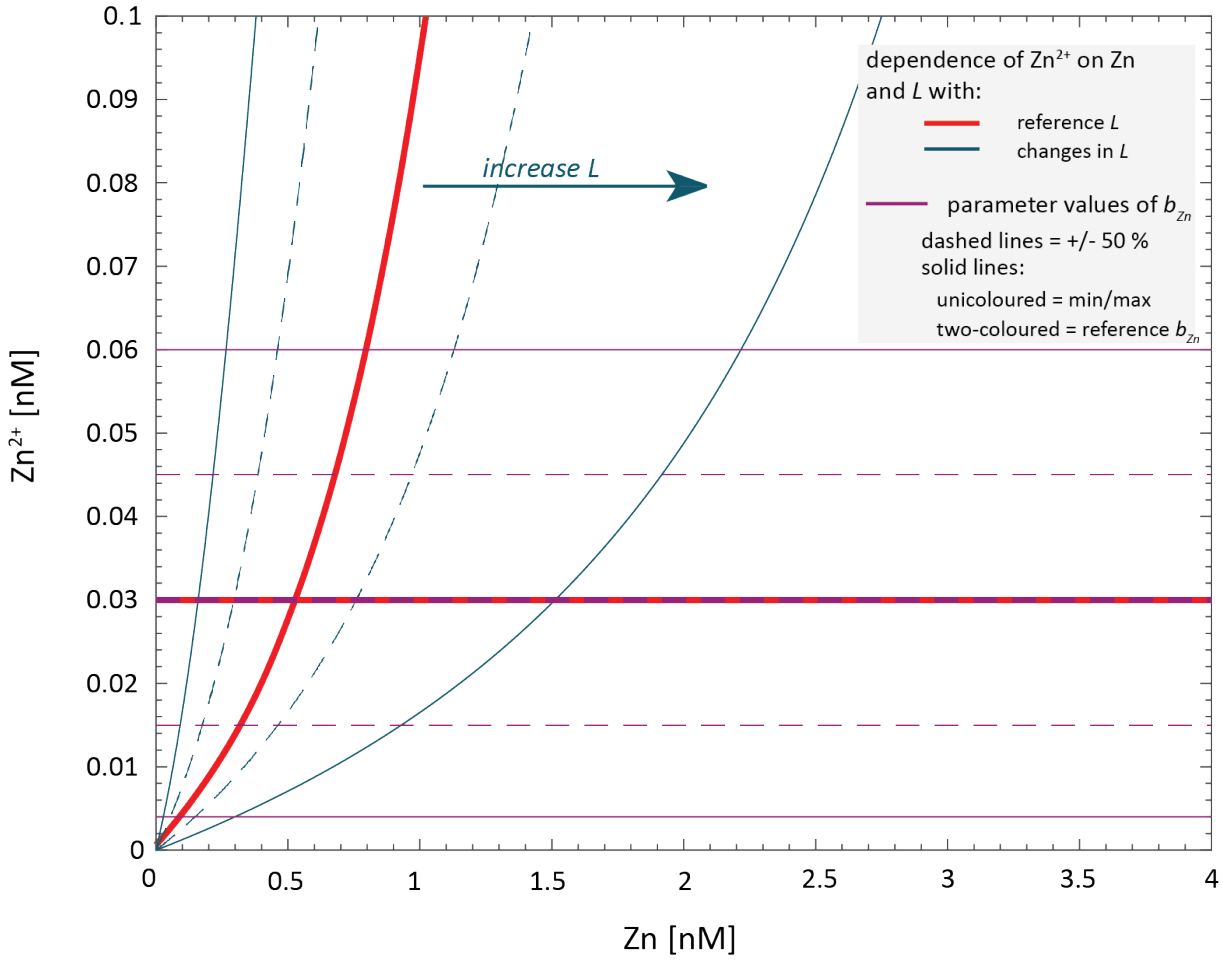

Figure S4. Concentration of Zn^{2+} versus total Zn calculated with reference values of b_{Zn} and L (red lines), and changes in each of these two parameters in turquoise and purple respectively.

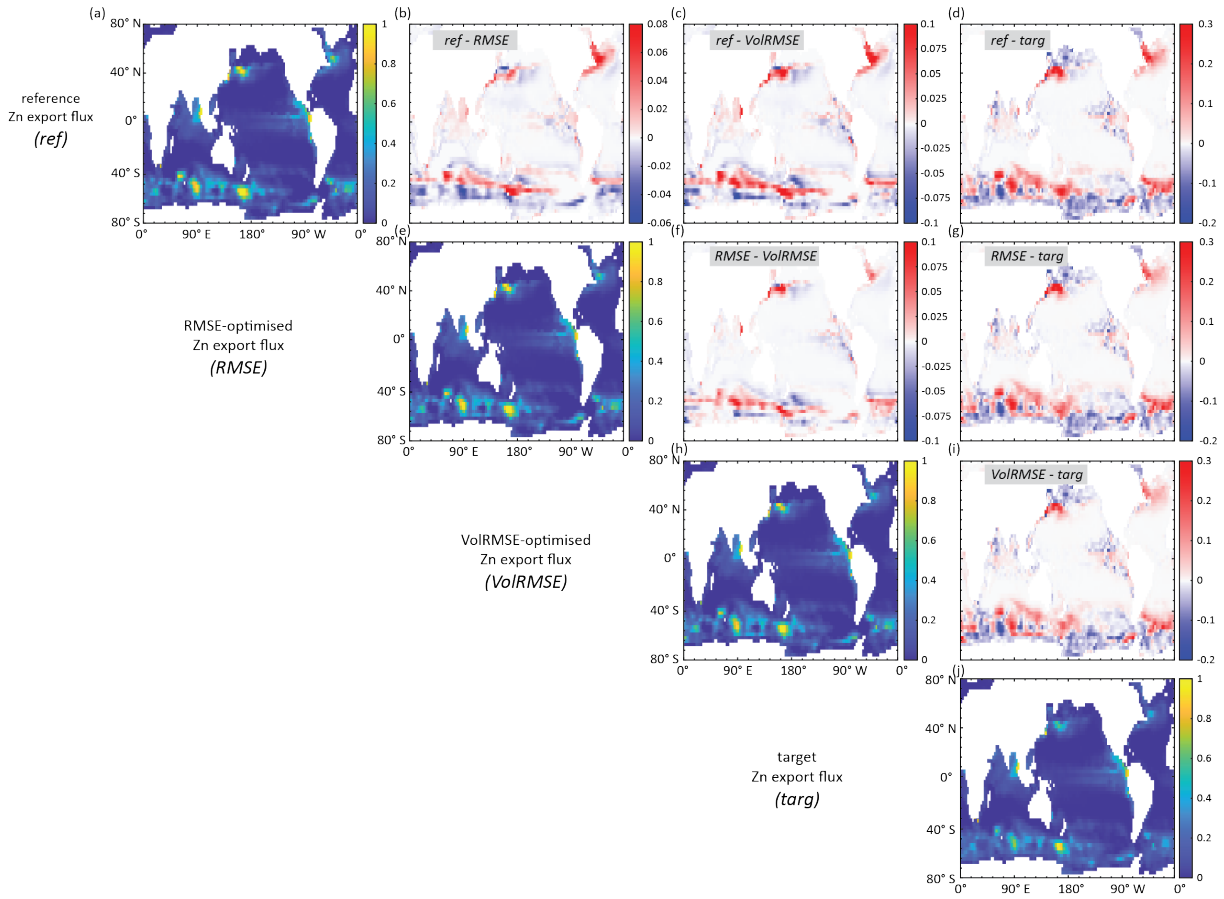

Figure S5. Global maps of annual Zn flux across the base of the euphotic zone (z_e=120m), obtained with **(a)** the reference parameters, **(e)** the RMSE-optimised and **(h)** VolRMSE-optimised parameters from experiment synObs_ALL_seas, and **(j)** the reference parameters while simulating seasonal variability (target of synObs_seas experiments). The other panels show the differences obtained when subtracting the Zn export flux in the panel below from the panel on the left. Note the different color scales in each column when plotting difference.

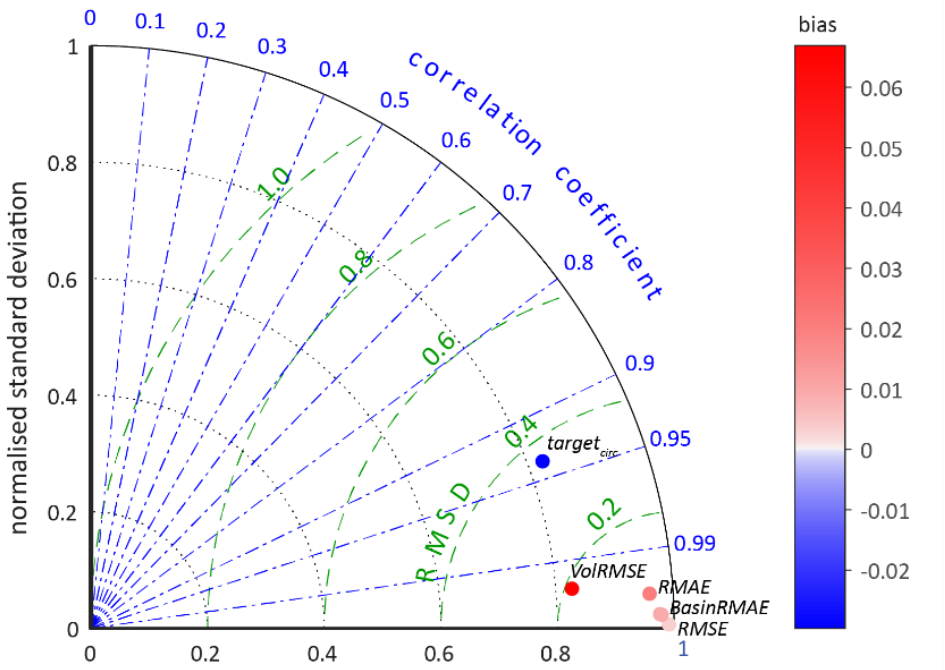

Figure S6. Taylor diagram comparing the target field applied in synObs_IDP_circ experiments ($target_{circ}$), and optimised fields obtained with different misfit functions in that experiment type, with the reference field. Even large differences in Zn uptake resulting from the very different uptake systematics of the VolRMSE-optimised experiment (Fig. 6f in the main text) cannot produce a Zn field as different from the reference field as the target field, which was produced with a different circulation model.

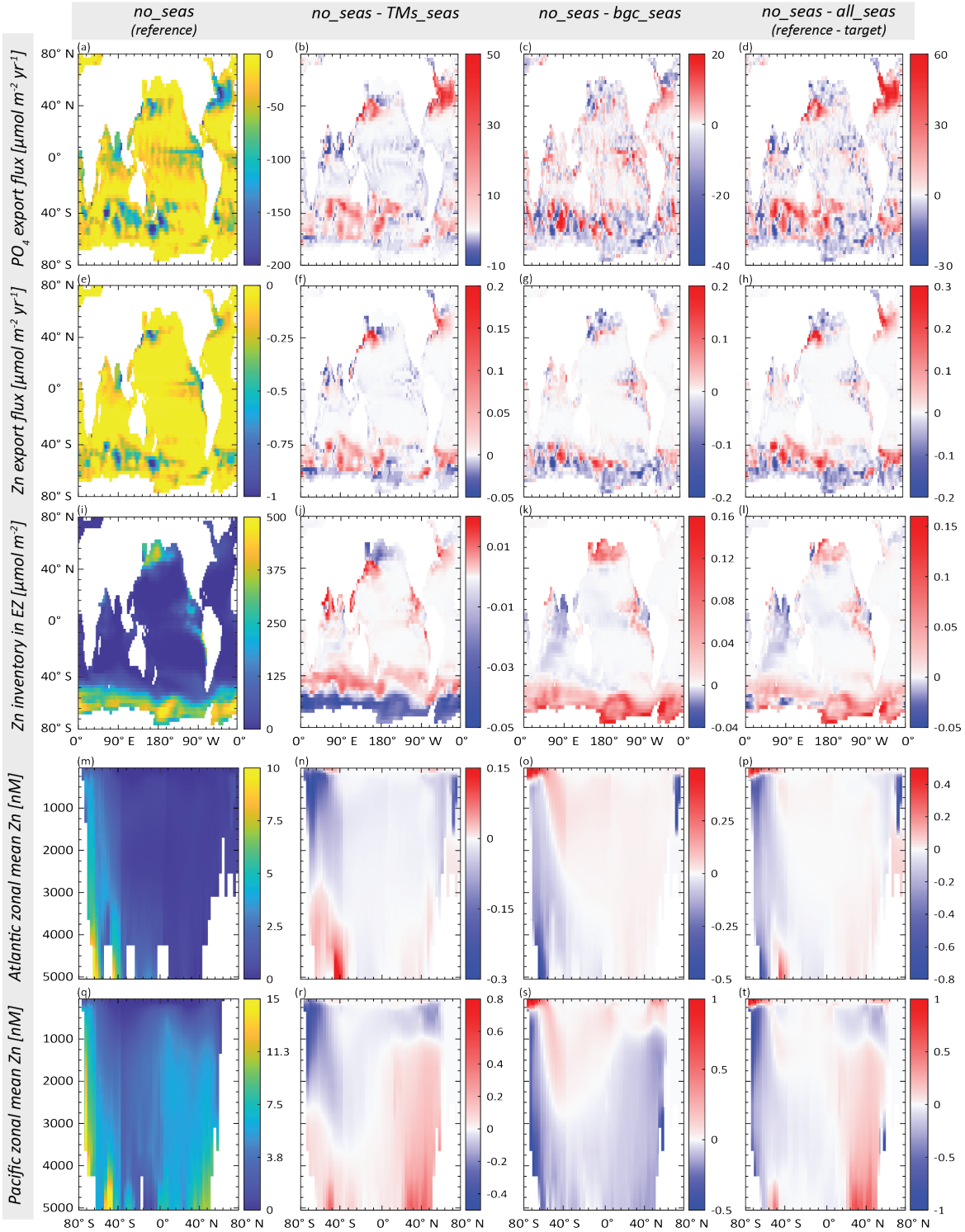

Figure S7. Influence of seasonality in circulation and biogeochemistry on Zn cycling and fields in MITgcm-2.8. The first column shows results obtained with the reference simulation, which uses annual mean TMs. The second, third, and fourth columns illustrate differences obtained when seasonality is simulated for either only circulation (monthly mean TMs; second column), only biogeochemistry only (restoring towards seasonal PO_4 fields; third column), or both simultaneously (target field for synObs_seas; fourth column). The first and second row visualise export fluxes for PO_4 and Zn respectively. The subsequent rows illustrate the (differences in) Zn inventory in the euphotic zone (third row), and zonal mean concentrations in the Atlantic (fourth row) and the Pacific (fifth row).

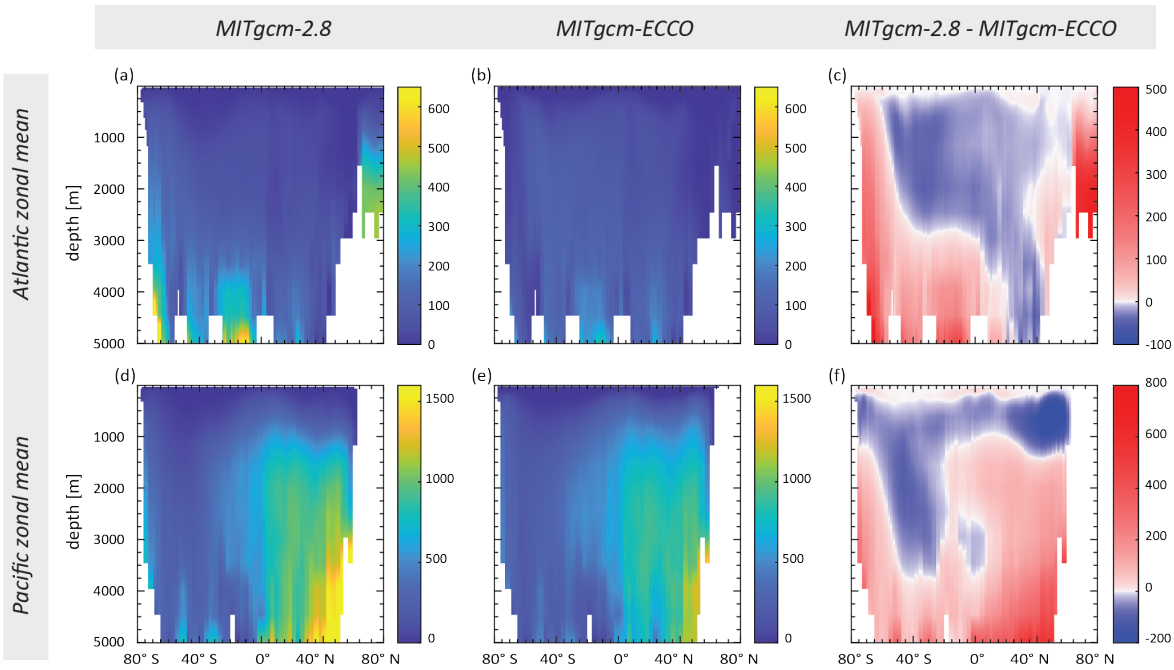

Figure S8. Ideal age (Thiele and Sarmiento, 1990) distribution in MITgcm-2.8 (first column) and MITgcm-ECCO (second column), zonally-averaged fields for the Atlantic (first row) and the Pacific (second row).

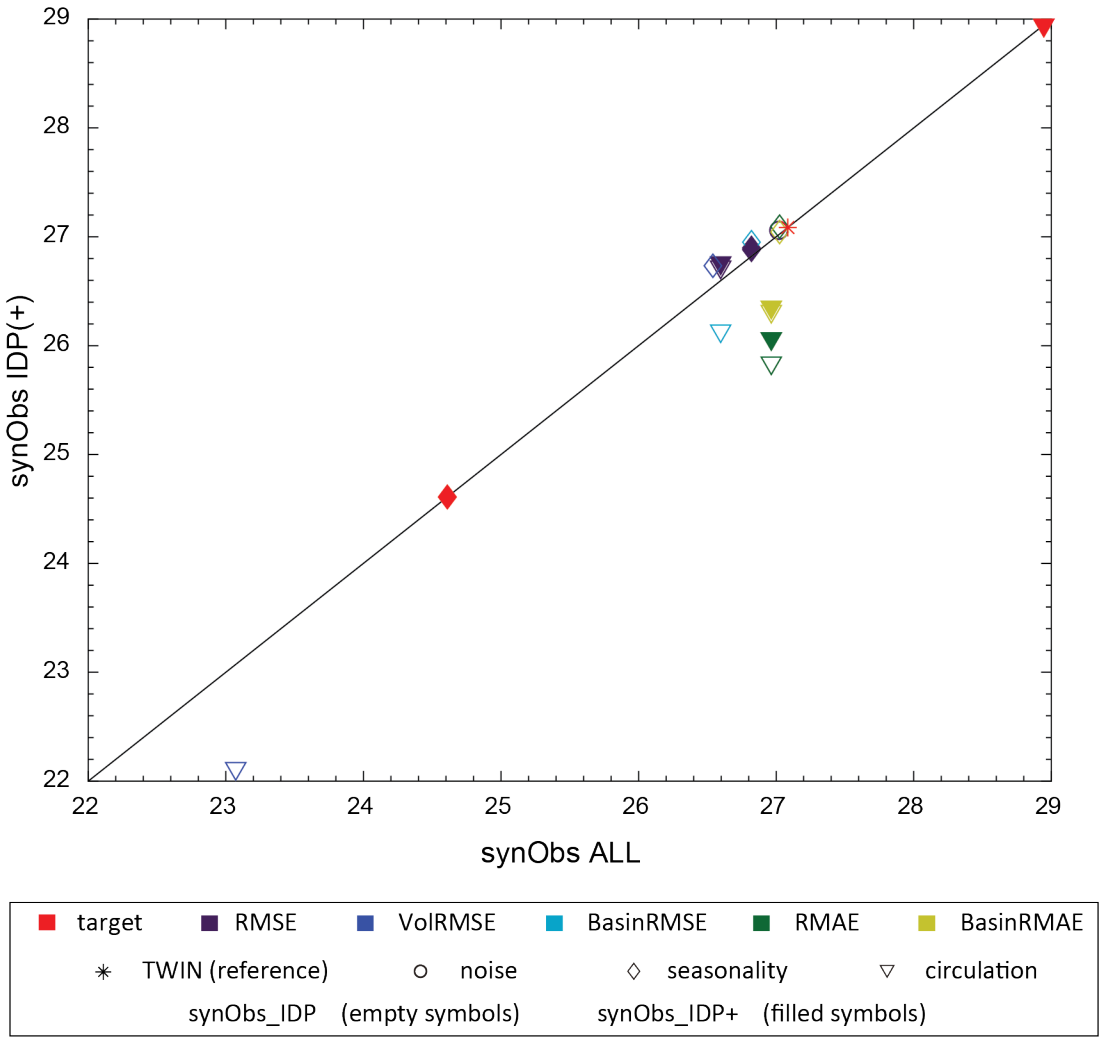

Figure S9. Integrated Zn export fluxes obtained in synObs_IDP(+) experiments vs. those obtained in the corresponding synObs_ALL experiments.

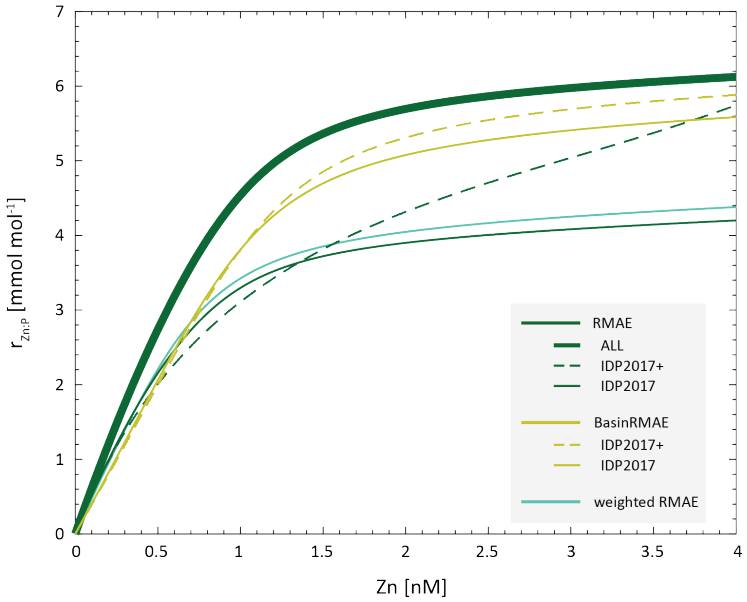

Figure S10. Optimised uptake systematics for synObs_IDP_circ obtained with a weighted RMAE (turquoise line), for which weights were determined based on the number of observations in IDP+ located in each ocean region used for BasinRMAE (Table S3). For comparison, the plot also shows RMAE-optimised uptake systematics obtained with synObs_ALL_circ (bold dark green line), synObs_IDP+_circ (dashed dark green line), and synObs_IDP_circ (solid dark green line), as well as BasinRMAE-optimised uptake systematics obtained with synObs_IDP+_circ (dashed light green line) and with synObs_IDP_circ (solid light green line).

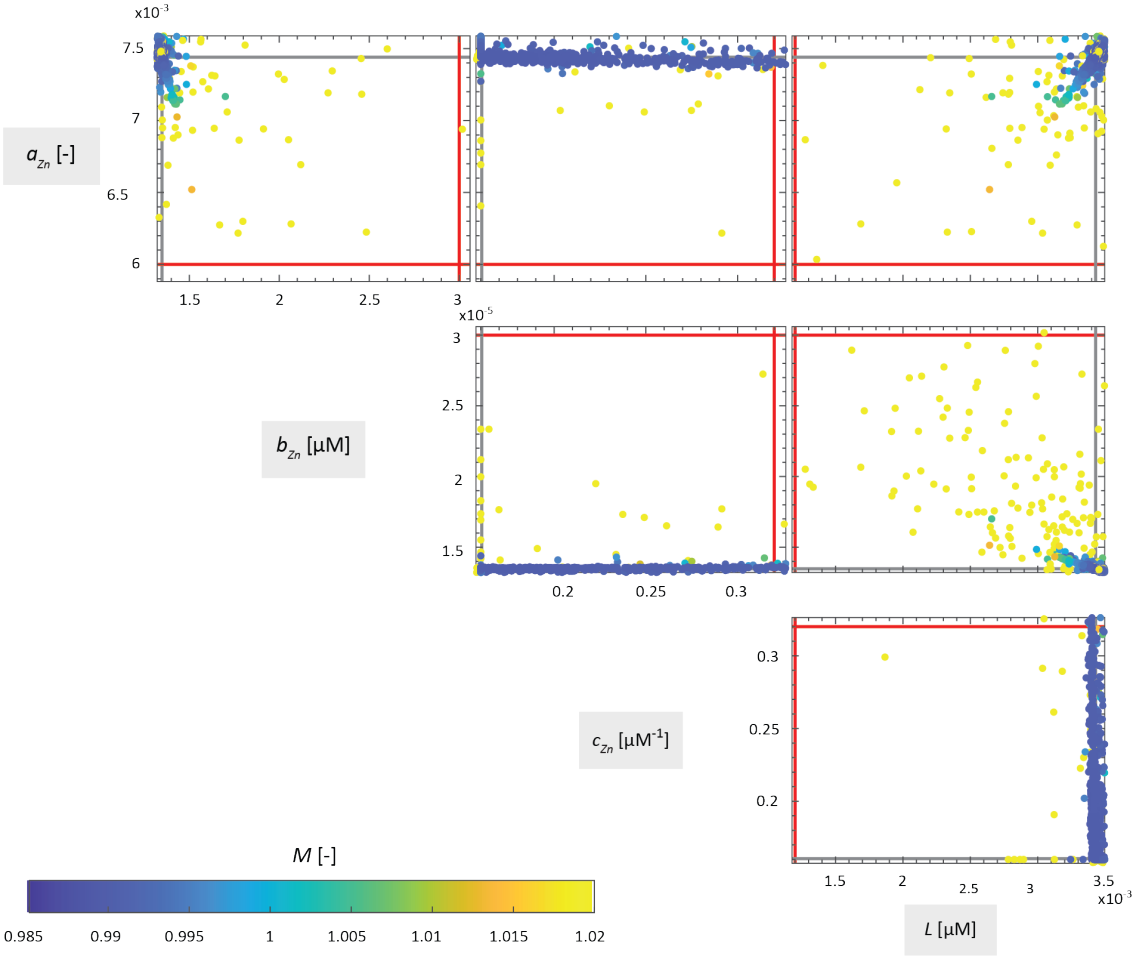

Figure S11. Misfit topography obtained in synObs_IDP_noise using VarRMSE misfit function. The misfit values are plotted for parameter regions covering ±2% of the optimised parameter value (grey line) and the reference value (red line).

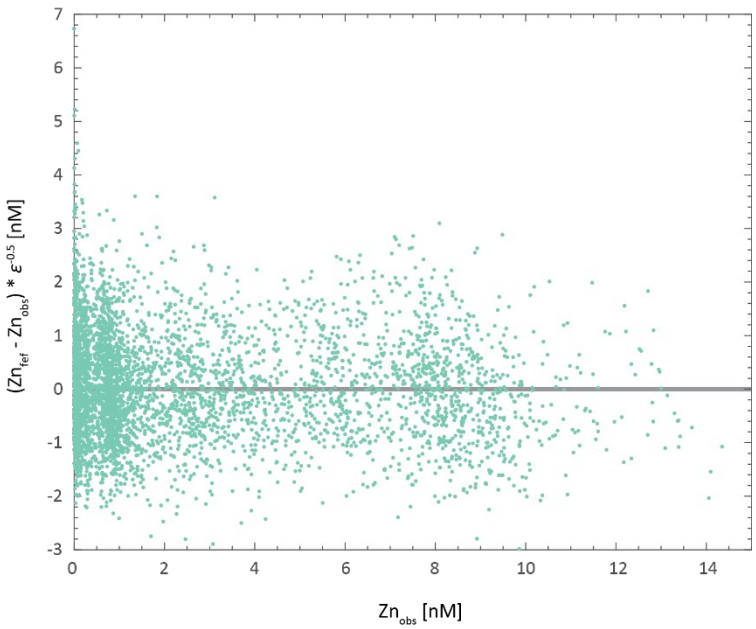

Figure S12. Standardised residuals between the reference field (Zn_{ref}) and the synObs_noise target field (Zn_{obs}). Note that the standard deviation $\varepsilon^{0.5}$ used for normalisation is based on Zn_{obs}, which itself is based on $\varepsilon(Zn_{ref})$.

References

Thiele, G. and Sarmiento, J. L.: Tracer dating and ocean ventilation, Journal of Geophysical Research: Oceans, 95, 9377-9391, https://doi.org/10.1029/JC095iC06p09377, 1990.